Atmos. Chem. Phys. Discuss., https://doi.org/10.5194/acp-2018-189
Manuscript under review for journal Atmos. Chem. Phys.
Discussion started: 13 April 2018

Atmospheric Chemistry and Physics Discussions

Differentiating between particle formation and growth events in an urban environment

Buddhi Pushpawela, Rohan Jayaratne, and Lidia Morawska*

International Laboratory for Air Quality and Health, Queensland University of Technology,

GPO Box 2434, Brisbane, QLD 4001, Australia

* Corresponding author contact details: Email: l.morawska@qut.edu.au

Abstract

Small aerosols at a given location in the atmosphere often originate in-situ from new particle formation (NPF). However, they can also be produced and then transported from a distant location to the point of observation where they may continue to grow to larger sizes. This study was carried out in the subtropical urban environment of Brisbane, Australia, in order to assess the relative occurrence frequencies of NPF events and particle growth events with no NPF. We used a neutral cluster and air ion spectrometer (NAIS) to monitor particles and ions in the size range 2-42 nm on 485 days, and identified 236 NPF events on 213 days. The majority of these events (37%) occurred during the daylight hours with just 10% at night. However, the NAIS also showed particle growth with no NPF on many nights (28%). Using a scanning mobility particle sizer (SMPS), we showed that particle growth continued at larger sizes and occurred on 70% of nights, typically under high relative humidities. Most

particles in the air, especially near coastal locations, contain hygroscopic salts such as sodium chloride that may exhibit deliquescence when the relative humidity exceeds about 75%. The growth rates of particles at night often exceeded the rates observed during NPF events. Although most of these night time growth events were preceded by daytime NPF events, the latter was not a prerequisite for growth. We conclude that particle growth in the atmosphere can be easily misidentified as NPF, especially when they are monitored by an instrument that cannot detect them at the very small sizes.

Keywords: New particle formation, particle growth, atmospheric aerosols, secondary particles.

1 Introduction

The formation of secondary particles in the atmosphere through homogeneous nucleation is known as new particle formation (NPF). This is one of the major sources of particles in the atmosphere. The condensable species that contribute are mainly sulfuric acid and semivolatile organic compounds and the process is thought to occur by binary water-sulfuric-acid or ternary water-sulfuric-acid-ammonia nucleation. Particles, thus formed, form stable clusters that continue to grow to larger sized particles by vapour condensation or by coagulation with other particles (Kulmala et al., 2013).

The particle formation rate and the particle growth rate are the two most important parameters used to characterize an NPF event. The particle formation rate is the rate of formation of smallest measurable size of the particles, generally in the size range 2-3 nm. This is different to the actual nucleation rate

(the rate at which the stable clusters form). The particle growth rate varies with particle size and, hence, the reported values depend on the detectable size ranges of the instruments used. Until recently, studies have been limited to measure the particles above 3 nm. However, it is only during the past decade that the advancement of instruments has developed to such a level that particles of 2 nm or even smaller can be measured (Kulmala et al., 2012).

NPF has been observed under a range of environmental conditions, on every continent in the world (Kulmala et al., 2004). The occurrence rate of NPF is mainly dependent on the nature and concentration of gaseous precursors, which are controlled by a number of factors including the type and intensity of the sources, concentration of pre-existing aerosols, origin of air masses, photo-chemical processes and meteorological parameters such as intensity of solar radiation, temperature, relative humidity, wind direction and wind speed (Birmili and Wiedensohler, 2000). Pre-existing aerosols act as sinks to condensable gases that are present in the atmosphere. This leads to a reduction in their vapour pressure and inhibits homogeneous nucleation.

Oxides of nitrogen and volatile organic compounds are readily produced in urban environments from sources such as motor vehicles and industrial facilities. These gases react with ozone in the presence of sunlight to produce OH radicals that can oxidise gaseous precursors such as sulphur dioxide and nitric oxide, converting them into the condensable species sulfuric acid and nitric acid, respectively. These

61 photochemical reactions are more likely to occur during the day time on sunny days with high intensity
62 of solar radiation, which is when we would expect to observe more NPF events.

63

64 Numerous studies in many different environments have conclusively shown that the large majority of
65 NPF occur during the day time. Very few studies have reported the occurrence of NPF during the night
66 time and these have mostly been in forest environments and coastal sites. Table 1 gives a summary of
67 studies in chronological order, that have reported observations and frequencies of occurrence of night
68 time NPF events, together with the respective frequencies of occurrence of day time NPF events and the
69 instrumentation that was used. We see that, at a given location, NPF events were generally more likely
70 to occur during the day time than during the night. The sole exception is the short study of 16 days by
71 Kammer et al. (2017). Night time events were reported on between 4% and 37% of the days observed.
72 They were more likely to be observed at forest locations (16% to 37%), while the two studies conducted
73 at coastal locations showed significantly lower values of 4% and 11%. In a previous study carried out in
74 and around Brisbane with an SMPS, Salimi et al. (2017) reported NPF events on around one in every
75 four nights. They also reported NPF on every second day which is significantly higher than any of the
76 values found in Brisbane (Guo et al., 2008;Cheung et al., 2011;Crilley et al., 2014;Jayaratne et al.,
77 2016;Pushpawela et al., 2018).

78

79 In the present study, we collected data of charged and uncharged particle concentrations in the urban
80 environment of Brisbane using a neutral cluster and air ion spectrometer (NAIS) on close to five
81 hundred days. The NAIS can provide more accurate information on NPF than the SMPS, because of its

ability to measure particles down to 2 nm in size, which is very close to the size at which the initial steps of nucleation and formation of particles occur (Manninen et al., 2011;Manninen et al., 2016). The results were compared with that obtained simultaneously with an SMPS with a minimum detectable size of 9 nm. The SMPS data were also used to determine the growth rates of particles. The observations by the NAIS and SMPS were used to differentiate between (a) local NPF events followed by particle growth and (b) growth events in the absence of NPF events – two phenomena that are not always concurrent and often misidentified when only one instrument is used.

Atmos. Chem. Phys. Discuss., https://doi.org/10.5194/acp-2018-189
Manuscript under review for journal Atmos. Chem. Phys.
Discussion started: 13 April 2018

2 Methods

2.1 Monitoring Site

The instruments were housed in a sixth-floor laboratory in a building at the Gardens Point campus of the Queensland University of Technology in Brisbane, Australia. The site is situated at the edge of the Brisbane Central Business District bordered by the City Botanical Gardens and the Brisbane River, approximately 100 m away from a busy motorway carrying about 120,000 vehicles per day and is representative of a typical urban environment in Australia. The measurements were carried out during the three calendar years 2012, 2015 and 2017, yielding 485 complete days of data.

The pollutants at this site were mainly from motor vehicle exhaust emissions. Depending on the wind direction, emissions may also be received from the Port of Brisbane and two oil refineries in its vicinity as well as from Brisbane Airport, all located about 20 km to the north-east of the monitoring site.

Meteorological data such as temperature, relative humidity, solar radiation, rainfall, wind direction and wind speed as well as air quality data such as sulphur dioxide (SO_2), ozone (O_3), PM_{10}, $PM_{2.5}$ and atmospheric visibility were obtained from the Department of Environmental and Heritage Protection, Queensland, at their in-situ site at the Queensland University of Technology and two other sites within a distance of 1.5 km from the University.

Atmos. Chem. Phys. Discuss., https://doi.org/10.5194/acp-2018-189
Manuscript under review for journal Atmos. Chem. Phys.
Discussion started: 13 April 2018

110 **2.2 Description of the instruments**

111 The NAIS, manufactured by Airel Ltd, Estonia (Manninen et al., 2016), detects the mobility distribution
112 of charged clusters and particles of both polarities in the electrical mobility range from 3.2 to 0.0013
113 $cm^2\ V^{-1}s^{-1}$. It also measures the size distribution of total particles in the size range from 2.0 - 42 nm. The
114 instrument has a high-resolution time down to 1 s and consists of two cylindrical electrical mobility
115 analysers, one for each polarity. It operates in four modes: ion mode; particle mode; alternate charging
116 mode and offset mode. In the ion mode, the NAIS measures naturally charged particles without any
117 modification. In the particle mode, it measures all charged and uncharged particles. The lower detection
118 limit in the particle mode is restricted to 2 nm due to presence of corona generated ions in the
119 instrument (Manninen et al., 2016). The alternate charging mode is similar to the particle mode, but it
120 electrically neutralizes the sampled particles and improves the performance of the instrument. In the
121 offset mode, the NAIS measures zero signals, noise levels and parasitic currents. The measurement
122 process of the instrument is fully automated. The measurement cycle of the NAIS varies from 2-5
123 minutes. A more detailed discussion of its design and principles is given in (Manninen et al., 2011) and
124 (Mirme and Mirme, 2013). In this study, we set the measurement cycle to 2 min ion mode, 2 min
125 particle mode, and 1 min offset mode.

126 An SMPS, consisting of a TSI model 3071 differential mobility analyser and a TSI model 3782
127 condensation particle counter, was used to measure the particle size distribution in the range from 9 -
128 415 nm.

129

Atmos. Chem. Phys. Discuss., https://doi.org/10.5194/acp-2018-189
Manuscript under review for journal Atmos. Chem. Phys.
Discussion started: 13 April 2018

Atmospheric Chemistry and Physics Discussions

130 **2.3 Data Analysis**

131 **2.3.1 Classification of New Particle Formation (NPF) events:**

132 We identified NPF events using the rate of change of total particle concentration, dN/dt, where N is the
133 number of particles in the size range 2.0 -10.0 nm and using the classification described by [Zhang et al
134 2004]. Events with N > 10,000 cm^{-3} for at least 1 hour and dN/dt >10,000 $cm^{-3}h^{-1}$ were defined as
135 "strong" NPF events. Events with 5000 < N < 10,000 cm^{-3} for at least 1 hour and 5000 < dN/dt < 10,000
136 $cm^{-3}h^{-1}$ were classified as "weak" NPF events. All of these events started in the nucleation mode size
137 range and prevailed over a time span of more than one hour, generally exhibiting a "banana" shape in
138 the time-series contour plot of particle number concentration (PNC), indicating particle formation and
139 subsequent growth. A 24-hour day that included at least one NPF event was labelled as an 'NPF Day'.
140 A day on which there were no NPF events was labelled as a 'Non-event Day'.

141 Every NPF event was characterised by a sharp increase of the PNC in the intermediate size range from
142 2.0-7.0 nm. This observation has been used to determine the starting time of an NPF event (Leino et al.,
143 2016). Similarly, in the present study, the starting time of a strong NPF event was determined by noting
144 the time of first occurrence of dN/dt > 10,000 $cm^{-3}h^{-1}$. The starting time of a weak NPF event was
145 determined by noting the time of first occurrence of dN/dt > 5000 $cm^{-3}h^{-1}$. N is the number of particles
146 in the size range 2.0-10 nm.

147 NPF events that started between 6:00 am and 6:00 pm were categorized as "day time" NPF. NPF events
148 that started between 6:00 pm and 6:00 am were categorized as "night time" NPF.

149

150 **2.3.2 Classification of Growth events:**

151 The data from the NAIS showed that growth events were not always preceded by an NPF event. Growth
152 events that did not follow an NPF appeared as a "floating-banana" shape in the PNC contour plots.
153 These events were identified using the rate of change in the diameter (d_p) of particle, dd_p/dt. Events with
154 $dd_p/dt > 1$ nm h^{-1} were classified as "growth" events. In the NAIS data, these events showed an
155 enhancement of PNC in the size range above 7 nm. Further, in these events, unlike in NPF events, the
156 sharp increase in PNC in the size range between 2-7 nm was absent. In this way, growth events could be
157 clearly distinguished from NPF events. In fact, unless they were preceded by an NPF event, most
158 growth events showed very few particles in the size range below 10 nm. We also observed "vertical
159 band" shapes which were due to the sudden appearance of high concentrations of particles in all sizes.
160 These were neither NPF nor growth events and characterised the influx of already formed particles from
161 further locations to the monitoring site, and were ignored in the analysis.

162

163 **2.3.3 Calculation of particles growth rate**

164 The growth rate (GR) of particles is defined as

165 $$\boldsymbol{GR} = \frac{\boldsymbol{dd_p}}{\boldsymbol{dt}} = \frac{\boldsymbol{d_{p2} - d_{p1}}}{\boldsymbol{t_2 - t_1}} \qquad (1)$$

166 where dp_2 and dp_1 are the diameters of particles at times t_1 and t_2. This was calculated by the maximum
167 concentration method described in (Kulmala et al., 2012). The unit of the GR is nanometres per hour.
168 During an NPF or a growth event, the number concentration of small particles increases, showing a

peak in the particle size distribution. When the particles grow in size, this peak shifts towards larger sizes. In order to derive the maximum particle concentration, we plotted the time series of the PNC in different size ranges. We estimated the GR from the slope of the best-fitted line on the graph of mid-point diameter of particles versus the time of maximum concentration (Dos Santos et al., 2015;Pierce et al., 2014).

2.3.4 Statistically significant differences

Statistical significances of the difference between two parameters were calculated using the Student's t test.

Atmos. Chem. Phys. Discuss., https://doi.org/10.5194/acp-2018-189
Manuscript under review for journal Atmos. Chem. Phys.
Discussion started: 13 April 2018

178 ## 3. Results and Discussion

179

180 ### 3.1 Observation of NPF during study period

181

182 The study yielded complete 24h data on a total of 485 days. The instrument was unavailable on some
183 days, as it was required for other projects or was being serviced or cleaned. In addition, a few days were
184 'lost' due to missing data owing to power failures or instrument malfunction. A summary of the
185 observational periods, together with the corresponding number of days on which 24h data were
186 available and NPF events were observed, is shown in Table 2. Columns 3 to 8 represent the number of
187 day time, night time and total NPF classified into strong and weak events according to the method
188 described in section 2.3.1. The last three columns give a summary of all NPF events.

189

190 Altogether, 236 NPF events (strong and weak) were observed on 213 of the 485 days on which we were
191 able to obtain data. Out of this, strong NPF events were observed on 177 days, giving an occurrence rate
192 of 37%. This is only slightly less than the rate of 41% found by Pushpawela et al. (2018) using the
193 NAIS in Brisbane over the single calendar year 2012. In the two other studies using the NAIS in
194 Brisbane, Crilley et al. (2014) and Jayaratne et al. (2016) reported higher values of 56% and 45%
195 respectively. However, both these previous studies used a slightly different criteria to identify NPF
196 events, that is they excluded the requirement of $N > 10{,}000\ cm^{-3}$ for a period of at least 1 hour. The
197 Crilley et al. (2014) study was also conducted over a much shorter period of 36 days only. Table 2 also
198 shows that, although "strong" day time NPF events were observed on 159 days (33%), "strong" night

time NPFs were relatively scarce, occurring on just 18 days (4%). Further, "weak" NPF events were observed on 59 days (12%) and these were almost equally distributed between night and day times. Taking into account all strong and weak NPF, day time NPF occurred on 37% of the days while night time NPF occurred on only 10%. In Table 2, it should be noted that a given day may sometimes have both a day time and a night time event. There were 23 such days. In addition, there were 8 days that had two daytime events and no instances of two events during the same night. There have been three previous studies that have used an SMPS to study NPF in Brisbane. Together with the occurrence rates in parenthesis, these were Guo et al. (2008) (35%), Cheung et al. (2011) (26%) and Salimi et al. (2017) (77%).

3.2 Diurnal variation

Figure 1 (a) shows a summary of starting times of all NPF events, estimated by using the method described in Section 2.3.1. Figure 1 (b) shows the histogram of number of events observed in each 30 min period of the day. Both of these figures show that most NPF events (73%) began during the morning, with a high likelihood of occurrence between 8.00 am and 10.00 am. In particular, 85 out of 236 events occurred during this 2-hour period. This is likely to be a result of several factors such as the higher concentration of precursor gases from motor vehicles during the morning rush hour and the onset of solar radiation. However, no NPF were observed during the evening rush hour period around 4-6 pm. During this time, the air temperatures are still relatively high and, although the gaseous precursors are being produced, the vapour pressures may not be sufficiently high to produce secondary particles. The

starting times of night time NPF events also showed a distinct trend with a peak likelihood between 8 and 9 pm. By this time of the day, the temperatures have generally fallen sufficiently for vapour pressures to increase. No night time events were observed at all during the second half of the night, between 11 pm and 4 am. Although the temperatures are low during this time, there is minimum production of precursor gases.

3.3 Effect of atmospheric parameters

A summary of the mean and range of various meteorological and air quality parameters during NPF and non-event days is shown in Table 3. The mean solar radiation intensity on NPF days were significantly higher compared to the other days with mean values of 505 W m^{-2} and 397 W m^{-2}, respectively. Conversely, the mean relative humidity on NPF days was significantly less than on other days with values of 54% and 66%, respectively. The mean relative humidity on NPF days were 59% and 52% during winter and summer months. Therefore, NPF events were more likely to occur on days with low relative humidity and high solar radiation. Similar observations have been reported from several other urban cites such as Melpitz, Germany (Birmili and Wiedensohler, 2000), San Pietro Capofiume, Italy (Hamed et al., 2007) and Pune, India (Kanawade et al., 2014).

The wind direction on NPF days was mainly from the south to southwest directions, with a mean wind speed of around 0.5 m s^{-1}. The mean air temperature was 17^0C and 24^0C on NPF days during winter and summer months. We did not detect any clear differences in wind direction, wind speed and air

241 temperature between NPF days and the other days. In general, most of the NPF events occurred on days
242 when there was no rainfall observed. However, a clear dependence was found between NPF occurrence
243 and atmospheric visibility. The visibility was expressed through the particle back scatter coefficient
244 (BSP) in units of Mm^{-1}. These two parameters are inversely proportional to each other. The BSP
245 observed at 8 am on NPF days was significantly lower on NPF days than on other days, with mean
246 values of 18 $Mm^{-1}$and 31 Mm^{-1}, respectively. A good discussion about the relationship between the
247 occurrence of NPF in Brisbane and the values of BSP may be found in Jayaratne et al. (2015). This
248 study also found that, no NPF events occurred on days when the mean $PM_{2.5}$ exceeded 20 μg m^{-3} in
249 Brisbane.
250
251 The presence of high concentration of O_3 under high solar radiation increases the production of OH
252 radicals, and the presence of high concentration of both SO_2 and OH radicals give rise to increased
253 production of H_2SO_4 leading to NPF (Seinfeld and Pandis, 2006;Lee et al., 2008). Therefore, we would
254 expect SO_2 and O_3 concentration levels to be higher on NPF days than on non-event days. However, we
255 observed only a marginal increase of SO_2 and O_3 concentrations on NPF days (Table 3).
256
257 **3.4 Day time and night time NPF events**
258
259 The two upper panels in Figure 2 show the NAIS spectragrams obtained between 8:00 am and 4:00 pm
260 on 19 August 2017 and 31 July 2015, respectively. On 19 August, a strong NPF event began in the
261 morning at around 9:00 am and lasted for 4-5 hours. Here, the total PNC increased from about 30,000

262 cm^{-3} at 9:00 am to just over 90,000 cm^{-3} at 11:00 am, giving a particle formation rate of 30,000 cm^{-3} h^{-1}.
263 Thereafter, particles continued to grow in size for several hours. The PNC decreased gradually in the
264 afternoon. The particles showed a relatively high growth rate of about 7 nm h^{-1} in the size range 2-42
265 nm.
266
267 The two lower panels in Figure 2 show NAIS spectragrams obtained during the night, between 6:00 pm
268 and 2:00 am on 20 August 2015 and 5 September 2015, respectively. On 20 August, a strong NPF event
269 began in the night at around 9:30 pm and lasted for 2-3 hours. The particles also showed a relatively
270 high growth rate of about 11 nm h^{-1} in the size range 2-42 nm.
271
272 We did not observe a significant difference in growth rates of particles between daytime and night time
273 NPF events. Typically, the growth rates were high during the first few hours and then decreased to a
274 few nanometres per hour within 3-4 hours after nucleation. The growth rate of particles in the size range
275 2-42 nm during all NPF events, calculated from equation (1), varied between 4 nm h^{-1} and 22 nm h^{-1}
276 with a mean and standard deviation of (12.1 ± 6.5) nm h^{-1}.
277
278 These growth rates were comparable to the values reported at two other urban locations; Atlanta, USA
279 (3-20 nm h^{-1})(Stolzenburg et al., 2005) and Budapest, Hungary (2-13 nm h^{-1}) (Salma et al., 2011).
280 However, the mean values of growth rates obtained by previous studies in Brisbane were significantly
281 lower than the value reported by this study. For example, Cheung et al. (2011) and Salimi et al. (2017)
282 reported growth rates of 4.6 nm h^{-1} and 2.4 nm h^{-1} respectively. Both these studies were carried out
283 using an SMPS with a lower detection size of about 10 nm.

Atmos. Chem. Phys. Discuss., https://doi.org/10.5194/acp-2018-189
Manuscript under review for journal Atmos. Chem. Phys.
Discussion started: 13 April 2018

Atmospheric Chemistry and Physics Discussions

284

285 **3.5 Observations of growth events during the study period**

286

287 NPF events are almost always followed by particle growth. However, with the NAIS, we observed
288 several growth events that were not preceded by an NPF event. These events were observed more often
289 at night than during the day. A summary of these events observed by the NAIS, is shown in Table 4.
290 Columns 3 to 5 represent the number of day time, night time and total growth events classified
291 according to the method described in section 2.3.2. Figure 3 shows examples of NAIS spectragrams of
292 such growth events that occurred during the day time (a) and night time (b). Particle growth is again
293 demonstrated by the typical banana shape of the colour contours, with the difference that the lower end
294 of the 'banana' does not reach as far as the smallest particle sizes, indicating that there is no NPF. This
295 shape is sometimes referred to as a "floating banana", to differentiate it from the complete "banana"
296 shape of an NPF event. In most of the events, particle growth is observed to continue for several hours.
297 The observed rates of growth varied between 1 nm h^{-1} and 45 nm h^{-1} with a mean and standard
298 deviation of (16.8 ± 11.9) nm h^{-1} in the size range 8-42 nm. During the 485 days of observation,
299 excluding NPF events, day time growth events were observed on just 54 days (11%), whereas night
300 time growth events were observed on 135 days (28%). The overall occurrence rate of growth events
301 obtained by the NAIS was 37%. However, it should be noted that particles continued to grow at sizes
302 larger than the upper size detection rate of the NAIS, which was 42 nm. Thus, the SMPS was likely to
303 detect many more growth events than the NAIS.

304

Atmos. Chem. Phys. Discuss., https://doi.org/10.5194/acp-2018-189
Manuscript under review for journal Atmos. Chem. Phys.
Discussion started: 13 April 2018

305 **3.6 Observations of particle growth by SMPS**

306

307 Next, we look at the behaviour of total PNC and the median particle diameter of NPF and growth events
308 using the data obtained by the SMPS. Figure 4 shows a period of 6 days, during which there were 3
309 consecutive daytime NPF events that were followed by two non-event days and a day with a daytime
310 NPF event. The NPF events are shown by red arrows. In each of these four cases, prior to the inception
311 of the daytime NPF, the total PNC was low - about 2500 cm^{-3}. During the NPF event, the total PNC
312 increased from about 5000 cm^{-3} in the morning to over 15,000 cm^{-3} near mid-day. Thereafter, the
313 particles started to grow in size up to 20-30 nm. During and after the late afternoon, although the total
314 PNC began to decrease, the particles continued to grow in size up to 40-65 nm. All 4 NPF events
315 continued through this "second phase of particle growth" until the early morning of the next day. The
316 growth rate varied between 2-7 nm h^{-1}.
317 Figure 5 shows another example. During this 7 day period, two growth events in the late afternoon were
318 preceded by NPF events. The remaining two growth events did not follow any NPF event. The particles
319 grew up to 40-50 nm. During the measurement period, particle growth events were observed on 65-
320 70% of the nights.

321

322 Continued growth of particles following NPF events have been reported by other researchers. For
323 example, Man et al. (2015) observed 12 out of 17 NPF events with particle growth from 10 nm to 40
324 nm during the day time at a suburban coastal site in Hong Kong. In addition, they observed 3 events
325 with second phase of particle growth to 61-97 nm at night time. These three events were preceded by a

daytime NPF event. Russell et al. (2007) observed nanoparticle growth on 19 out of 48 days (40%) during the day time and on 5 out of 48 days (10%) during the night time in Appledore Island, Maine, USA. Subsequently, particle growth continued over several hours with rates varying from 3 to 13 nm h^{-1}.

NPF generally occur at high solar radiation, high temperature and low relative humidity. However, growth events were more likely to occur during time periods with low temperature and high relative humidity. We investigated this further by plotting the median particle size and relative humidity as a function of time during growth events (Figure 6). In general, progression into the night time, after 6:00 pm, was accompanied by a decrease in air temperature, resulting in an increase in relative humidity in the atmosphere.

During the event that occurred on July 16, 2012 the median particle size increased from about 30 to 65 nm as the relative humidity increased from 65% to 80% (Figure 6a). Similarly, during the event that occurred on July 20, 2012 the median particle size increased from about 30 to 75 nm as the relative humidity increased from 75% to 90% (Figure 6b).

It is well-known that atmospheric aerosol particles change their size with relative humidity due to the uptake of water (Winkler, 1988). Water uptake is caused by the deliquescence of soluble salts which form a solution when the solid compound is exposed to water vapour at sufficiently high vapour pressure. Several organic materials are also known to absorb water at high humidity which is more

generally known as hygroscopicity. Figure 7 shows the diameter of a sodium chloride (NaCl)-bearing particle as a function of relative humidity (Wise et al., 2007). The red line corresponds to the deliquescence point for NaCl at 76% relative humidity. At this point, the particle deliquesces and becomes a solution of droplet with a well-defined spherical shape. The particle diameter does not change considerably as the relative humidity is increased from 0 to 74%. As the relative humidity increased from 76% to 91%, the particle diameter increased by a factor of 1 or more. Therefore, as the relative humidity increases, the particles sizes increase due to their affinity to absorb water. Close to the coast, sea-salt aerosols constitute a large proportion of the atmospheric particulate mass and NaCl is a major component. Many of the inorganic substances that readily absorb water, such as sea salt, ammonium salts and nitrates, are present in the Brisbane environment (Harrison, 2007). Therefore, it is not surprising that, in the present study, we observed that particle growth occurred on 7 out of 10 nights with high relative humidity.

3.7 Probability of growth events being misidentified as NPF events

In Figure 3 (a), the horizontal white line indicates the typical lower size detection threshold of the SMPS that has been used in many locations before; we chose 7 nm as a typical value in this case. The SMPS does not 'see' any particles below this line. It is clear that there is an enhancement of PNC in the size range 7-20 nm around 11:30 am on this day. The absence of intermediate size particles (between 2-7 nm) suggests that the 7-20 nm particles originated on-site by primary emission or were advected to the site from a distant location. The NAIS clearly shows that this was not an NPF event. However, in the

368 absence of information below a particle size of 7 nm, the SMPS data may be easily misinterpreted as an
369 NPF event. The typical 'floating banana' shape of the spectragram contours show that the particles
370 continue to grow between 11:30 a.m. and about 1:00 p.m. and this can be observed by an SMPS. As we
371 have demonstrated, growth events are not always formation events. There are two enhancement events
372 near 1.00 pm and 3.30 pm. Once again, the NAIS shows that neither of these are NPF events, although
373 based on the SMPS they may be mistakenly identified as such. Figure 3 (b) shows another event that
374 can be easily misidentified as an NPF event based on SMPS data alone.

375

376 Salimi et al. (2017), using an SMPS with a lower size limit of 9 nm at 25 sites across Brisbane, reported
377 219 NPF events out of 285 days of measurements. This occurrence rate of 77% (67% of day time and
378 33% of night time) is significantly higher than any of the values found previously in Brisbane and at
379 any other location in the world. With the NAIS, it was possible to show that most of these events were
380 growth events and not NPF events. It was not possible to differentiate these two types of events with the
381 SMPS alone as it provides no knowledge of the PNC below 9 nm. With the NAIS, we did not observe
382 nocturnal NPF events on more than 47 of 500 days.

383

384 In many NPF events, particle growth ceases after they have grown to a certain size. In the growth event
385 in Figure 3, the maximum size is about 25 nm. In such cases, the greater part of the 'banana' profile is
386 below 7 nm and, thus, invisible to the SMPS. This could result in the missing of such NPF events.

Considering, all the factors above, it is clear that the NAIS has a distinct advantage over the SMPS in correctly identifying NPF events in the atmosphere.

4. Summary and Conclusions

We monitored charged and neutral PNCs in the size range 2-42 nm on nearly 500 days over three calendar years in the urban environment of Brisbane, Australia, using a NAIS. The data were used to differentiate between NPF events and growth events with no NPF. Day time NPF events were observed on 37% of the observational days, with night time events on only 10% of the days. NPF events were more likely to occur on days with low relative humidity and high solar radiation. 73% of NPF events occurred during the morning, with the highest probability of occurrence between 8.00 am and 10.00 am. Most of the night time events occurred between 8.00 pm and 9:00 pm. No night time events were observed between 11.00 pm and 4.00 am. 28% of the particle growth events that occurred at night were not preceded by an NPF event. These events were characterized by high growth rates of up to 45 nm h^{-1}. The SMPS results showed that particle growth continued at larger sizes from ~40 nm to 70 nm and occurred on 70% of nights. Maximum relative humidities were over 80% on most of these nights. These results show that, when particles are monitored by an instrument such as the SMPS that cannot detect them at the very small sizes, particle growth in the atmosphere may be easily misidentified as NPF, leading to an overestimation of the frequency of the latter.

Acknowledgements

We are thankful to the Department of Environmental and Heritage Protection, Queensland, for providing some of the meteorological data used in this study.

References:

Birmili, W., and Wiedensohler, A.: New particle formation in the continental boundary layer: Meteorological and gas phase parameter influence, Geophysical Research Letters, 27, 3325-3328, 2000.

Cheung, H., Morawska, L., and Ristovski, Z.: Observation of new particle formation in subtropical urban environment, Atmospheric Chemistry and Physics, 11, 3823, 2011.

Crilley, L. R., Jayaratne, E. R., Ayoko, G. A., Miljevic, B., Ristovski, Z., and Morawska, L.: Observations on the formation, growth and chemical composition of aerosols in an urban environment, Environmental science & technology, 48, 6588-6596, 2014.

Dos Santos, V., Herrmann, E., Manninen, H., Hussein, T., Hakala, J., Nieminen, T., Aalto, P., Merkel, M., Wiedensohler, A., and Kulmala, M.: Variability of air ion concentrations in urban Paris, Atmospheric Chemistry and Physics, 15, 13717-13737, 2015.

Guo, H., Ding, A., Morawska, L., He, C., Ayoko, G., Li, Y. S., and Hung, W. T.: Size distribution and new particle formation in subtropical eastern Australia, Environ. Chem., 5, 382-390, 2008.

Hamed, A., Joutsensaari, J., Mikkonen, S., Sogacheva, L., Maso, M. D., Kulmala, M., Cavalli, F., Fuzzi, S., Facchini, M., and Decesari, S.: Nucleation and growth of new particles in Po Valley, Italy, Atmospheric Chemistry and Physics, 7, 355-376, 2007.

Harrison, R. M.: Understanding our environment: an introduction to environmental chemistry and pollution, Royal Society of chemistry, 2007.

Jayaratne, E. R., Clifford, S., and Morawska, L.: Atmospheric Visibility and PM10 as Indicators of New Particle Formation in an Urban Environment, Environmental Science & Technology, 49, 12751-12757, 10.1021/acs.est.5b01851, 2015.

Jayaratne, E. R., Pushpawela, B., and Morawska, L.: Temporal evolution of charged and neutral nanoparticle concentrations during atmospheric new particle formation events and its implications for ion-induced nucleation, Frontiers of Environmental Science & Engineering, 10, 13, 2016.

Junninen, H., Hulkkonen, M., Riipinen, I., Nieminen, T., Hirsikko, A., Suni, T., Boy, M., LEE, S. H., Vana, M., and Tammet, H.: Observations on nocturnal growth of atmospheric clusters, Tellus B, 60, 365-371, 2008.

Kalivitis, N., Stavroulas, I., Bougiatioti, A., Kouvarakis, G., Gagné, S., Manninen, H., Kulmala, M., and Mihalopoulos, N.: Night-time enhanced atmospheric ion concentrations in the marine boundary layer, Atmospheric Chemistry and Physics, 12, 3627-3638, 2012.

Kammer, J., Perraudin, E., Flaud, P.-M., Lamaud, E., Bonnefond, J., and Villenave, E.: Observation of nighttime new particle formation over the French Landes forest, Science of The Total Environment, 2017.

Kanawade, V., Tripathi, S. N., Siingh, D., Gautam, A. S., Srivastava, A. K., Kamra, A. K., Soni, V. K., and Sethi, V.: Observations of new particle formation at two distinct Indian subcontinental urban locations, Atmos. Environ., 96, 370-379, 2014.

447 Kulmala, M., Vehkamäki, H., Petäjä, T., Dal Maso, M., Lauri, A., Kerminen, V.-M., Birmili, W., and
448 McMurry, P. H.: Formation and growth rates of ultrafine atmospheric particles: a review of
449 observations, J. Aerosol Sci., 35, 143-176, 2004.
450 Kulmala, M., Petäjä, T., Nieminen, T., Sipilä, M., Manninen, H. E., Lehtipalo, K., Dal Maso, M., Aalto,
451 P. P., Junninen, H., and Paasonen, P.: Measurement of the nucleation of atmospheric aerosol particles,
452 Nature protocols, 7, 1651-1667, 2012.
453 Kulmala, M., Kontkanen, J., Junninen, H., Lehtipalo, K., Manninen, H. E., Nieminen, T., Petäjä, T.,
454 Sipilä, M., Schobesberger, S., and Rantala, P.: Direct observations of atmospheric aerosol nucleation,
455 Science, 339, 943-946, 2013.
456 Lee, S. H., Young, L. H., Benson, D. R., Suni, T., Kulmala, M., Junninen, H., Campos, T. L., Rogers,
457 D. C., and Jensen, J.: Observations of nighttime new particle formation in the troposphere, Journal of
458 Geophysical Research: Atmospheres (1984–2012), 113, 2008.
459 Leino, K., Nieminen, T., Manninen, H. E., Petäjä, T., Kerminen, V.-M., and Kulmala, M.: Intermediate
460 ions as a strong indicator of new particle formation bursts in a boreal forest, Boreal Environment
461 Research, 2016.
462 Man, H., Zhu, Y., Ji, F., Yao, X., Lau, N. T., Li, Y., Lee, B. P., and Chan, C. K.: Comparison of
463 daytime and nighttime new particle growth at the HKUST supersite in Hong Kong, Environmental
464 science & technology, 49, 7170-7178, 2015.
465 Manninen, H., Franchin, A., Schobesberger, S., Hirsikko, A., Hakala, J., Skromulis, A., Kangasluoma,
466 J., Ehn, M., Junninen, H., and Mirme, A.: Characterisation of corona-generated ions used in a Neutral
467 cluster and Air Ion Spectrometer (NAIS), Atmospheric Measurement Techniques, 4, 2767, 2011.

Manninen, H. E., Mirme, S., Mirme, A., Petäjä, T., and Kulmala, M.: How to reliably detect molecular clusters and nucleation mode particles with Neutral cluster and Air Ion Spectrometer (NAIS), Atmos. Meas. Tech. Discuss, 2016.

Mazon, S. B., Kontkanen, J., Manninen, H. E., Nieminen, T., Kerminen, V.-M., and Kulmala, M.: A long-term comparison of nighttime cluster events and daytime ion formation in a boreal forest, Boreal Environment Research, 2016.

Mirme, S., and Mirme, A.: The mathematical principles and design of the NAIS-a spectrometer for the measurement of cluster ion and nanometer aerosol size distributions, Atmospheric Measurement Techniques, 6, 1061, 2013.

Pierce, J., Westervelt, D., Atwood, S., Barnes, E., and Leaitch, W.: New-particle formation, growth and climate-relevant particle production in Egbert, Canada: analysis from 1 year of size-distribution observations, Atmospheric Chemistry and Physics, 14, 8647-8663, 2014.

Pushpawela, B., Jayaratne, R., and Morawska, L.: Temporal distribution and other characteristics of new particle formation events in an urban environment, Environmental Pollution, 233, 552-560, https://doi.org/10.1016/j.envpol.2017.10.102, 2018.

Russell, L., Mensah, A., Fischer, E., Sive, B., Varner, R., Keene, W., Stutz, J., and Pszenny, A.: Nanoparticle growth following photochemical α-and β-pinene oxidation at Appledore Island during International Consortium for Research on Transport and Transformation/Chemistry of Halogens at the Isles of Shoals 2004, Journal of Geophysical Research: Atmospheres, 112, 2007.

Salimi, F., Rahman, M., Clifford, S., Ristovski, Z., and Morawska, L.: Nocturnal new particle formation events in urban environments, Atmospheric Chemistry and Physics, 17, 521-530, 2017.

Salma, I., Borsós, T., Weidinger, T., Aalto, P., Hussein, T., Dal Maso, M., and Kulmala, M.: Production, growth and properties of ultrafine atmospheric aerosol particles in an urban environment, Atmospheric Chemistry and Physics, 11, 1339, 2011.

Seinfeld, J.H., Pandis, S.N., 2006. Atmospheric Chemistry and Physics. Wiley, Hoboken, NJ.

Stolzenburg, M. R., McMurry, P. H., Sakurai, H., Smith, J. N., Mauldin, R. L., Eisele, F. L., and Clement, C. F.: Growth rates of freshly nucleated atmospheric particles in Atlanta, Journal of Geophysical Research: Atmospheres, 110, 2005.

Suni, T., Kulmala, M., Hirsikko, A., Bergman, T., Laakso, L., Aalto, P., Leuning, R., Cleugh, H., Zegelin, S., and Hughes, D.: Formation and characteristics of ions and charged aerosol particles in a native Australian Eucalypt forest, Atmospheric Chemistry and Physics, 8, 129-139, 2008.

Svenningsson, B., Arneth, A., Hayward, S., Holst, T., Massling, A., Swietlicki, E., Hirsikko, A., Junninen, H., Riipinen, I., and Vana, M.: Aerosol particle formation events and analysis of high growth rates observed above a subarctic wetland–forest mosaic, Tellus B, 60, 353-364, 2008.

Winkler, P.: The growth of atmospheric aerosol particles with relative humidity, Physica Scripta, 37, 223, 1988.

Wise, M. E., Semeniuk, T. A., Bruintjes, R., Martin, S. T., Russell, L. M., and Buseck, P. R.: Hygroscopic behavior of NaCl-bearing natural aerosol particles using environmental transmission electron microscopy, Journal of Geophysical Research: Atmospheres, 112, 2007.

Atmos. Chem. Phys. Discuss., https://doi.org/10.5194/acp-2018-189
Manuscript under review for journal Atmos. Chem. Phys.
Discussion started: 13 April 2018

Atmospheric Chemistry and Physics Discussions

509 **Figures**

510

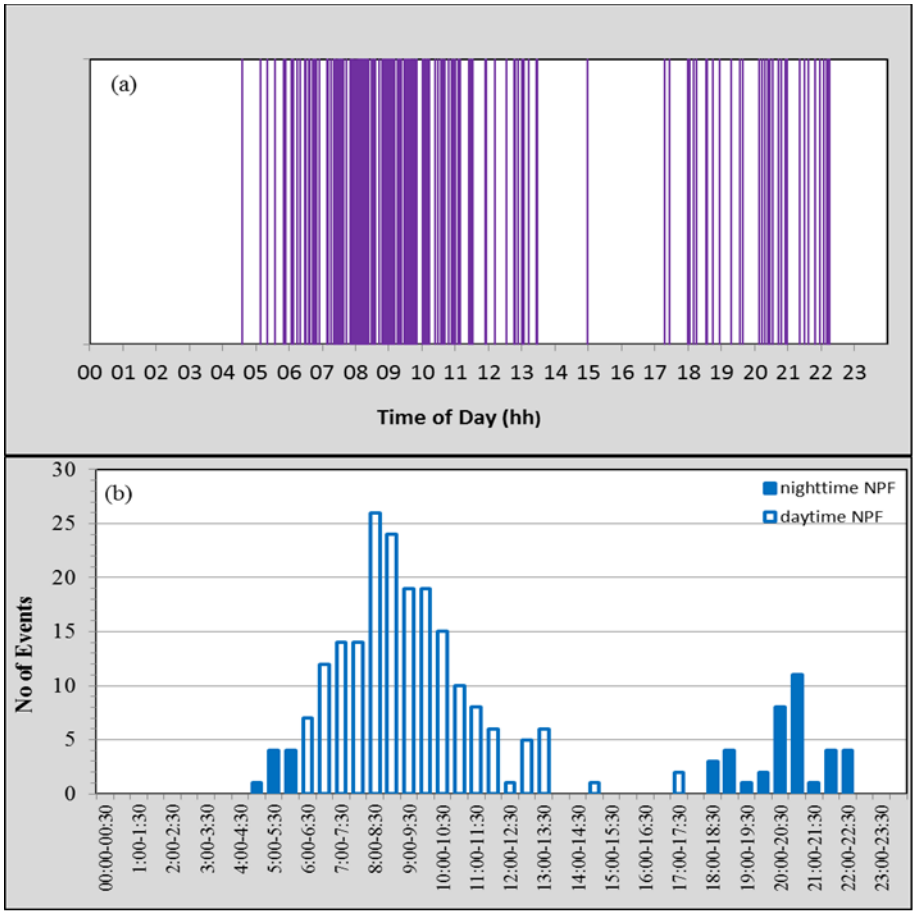

511

512 Figure 1: (a) Summary of starting times of all NPF events and (b) histogram for the number of events

513

Atmos. Chem. Phys. Discuss., https://doi.org/10.5194/acp-2018-189
Manuscript under review for journal Atmos. Chem. Phys.
Discussion started: 13 April 2018

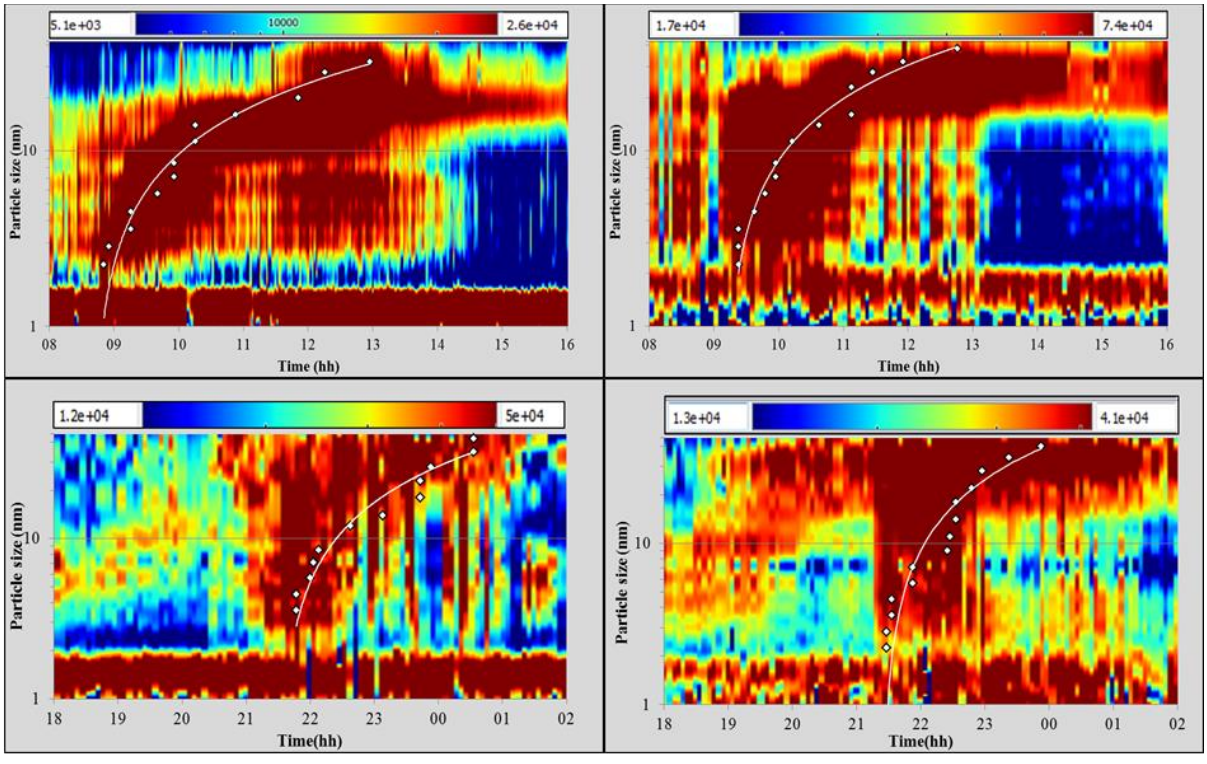

514

515 Figure 2: NAIS spectragrams of the daytime NPF events (upper panel) and nighttime NPF (lower
516 panel). The colour contour represents the PNC and the markers represent the times at which the PNC
517 reached its maximum value at each particle size. The unit of PNC is per cubic centimetre. Data below 2
518 nm should be treated with caution due to instrumentation limitations as described in the text.

519

520

521

522

523

524

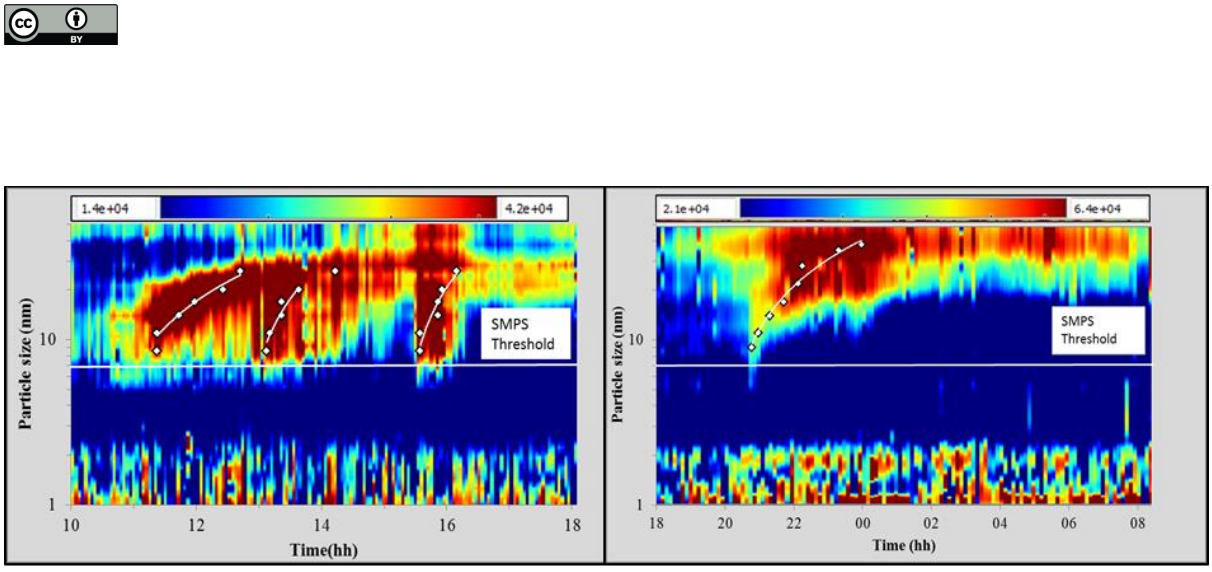

Figure 3: NAIS spectragrams of the growth events that occurred during (a) day time (b) night time. Note the "floating banana" shape which indicates that these are clearly not NPF events. The SMPS cannot detect particles at sizes below the horizontal white line. The colour contour represents the PNC and the markers represent the times at which the PNC reached its maximum value at each particle size. The unit of PNC is per cubic centimetre.

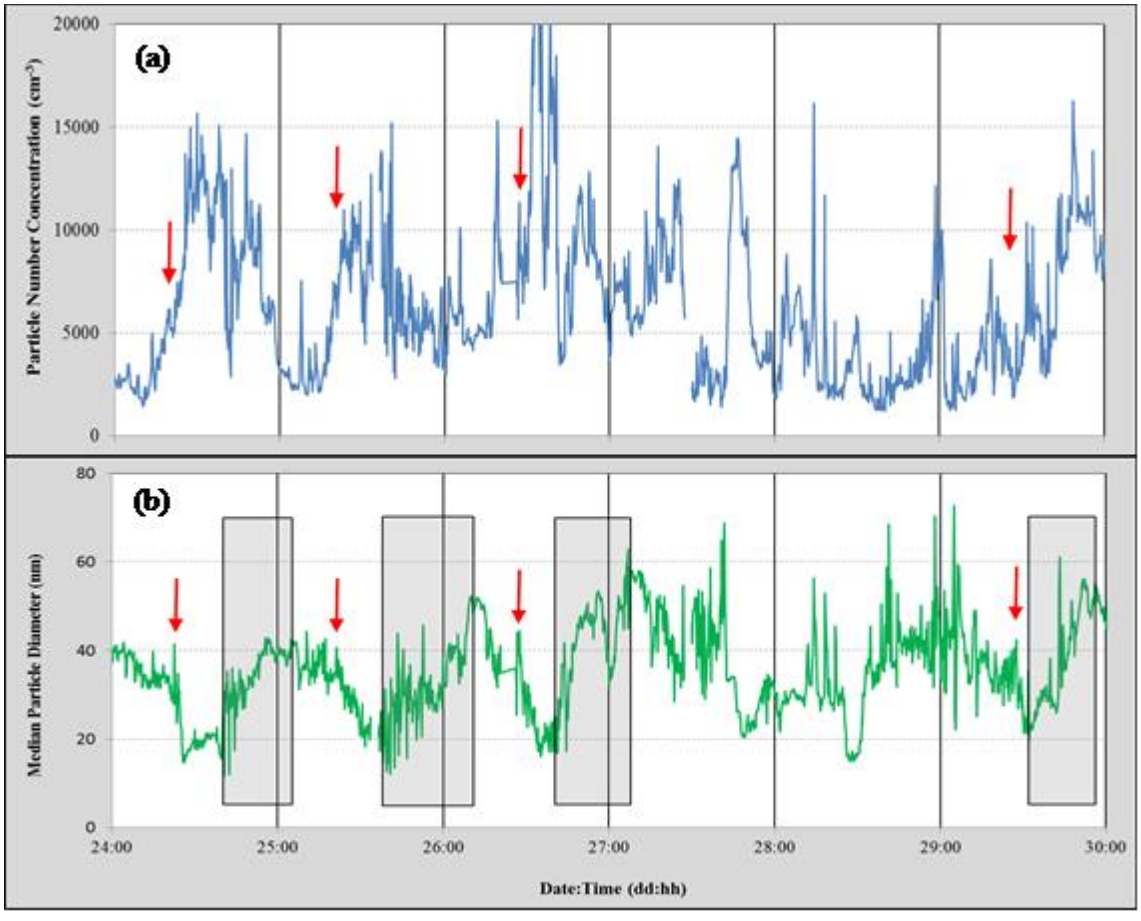

Figure 4: (a) the total PNC and (b) median particle diameter from the SMPS during 24 July-30 July, 2012. Red arrows and gray boxes represent the day time NPF events and the growth events, respectively.

Atmos. Chem. Phys. Discuss., https://doi.org/10.5194/acp-2018-189
Manuscript under review for journal Atmos. Chem. Phys.
Discussion started: 13 April 2018

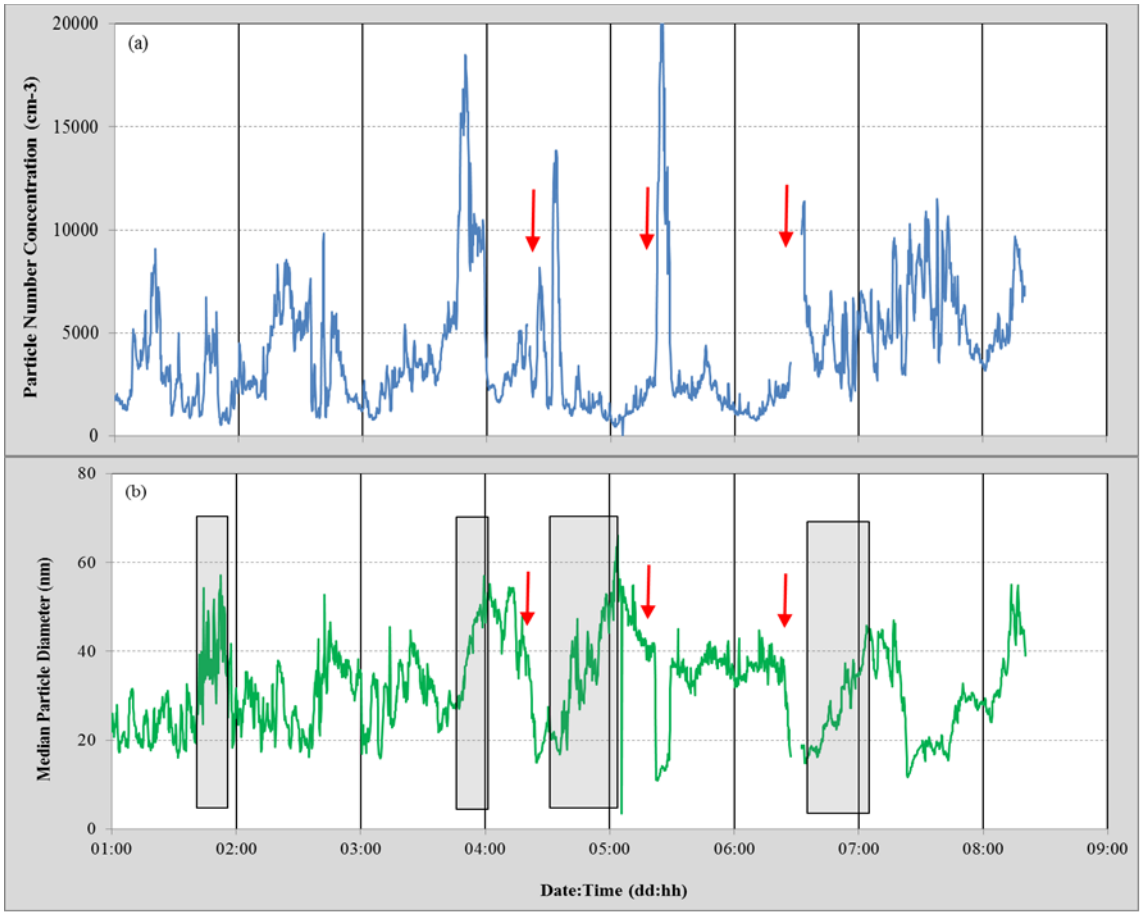

Figure 5: (a) the total PNC and (b) median particle diameter from the SMPS during 1 June-7 June, 2012. Red arrows and gray boxes represent the daytime NPF events and the growth events, respectively.

Atmos. Chem. Phys. Discuss., https://doi.org/10.5194/acp-2018-189
Manuscript under review for journal Atmos. Chem. Phys.
Discussion started: 13 April 2018

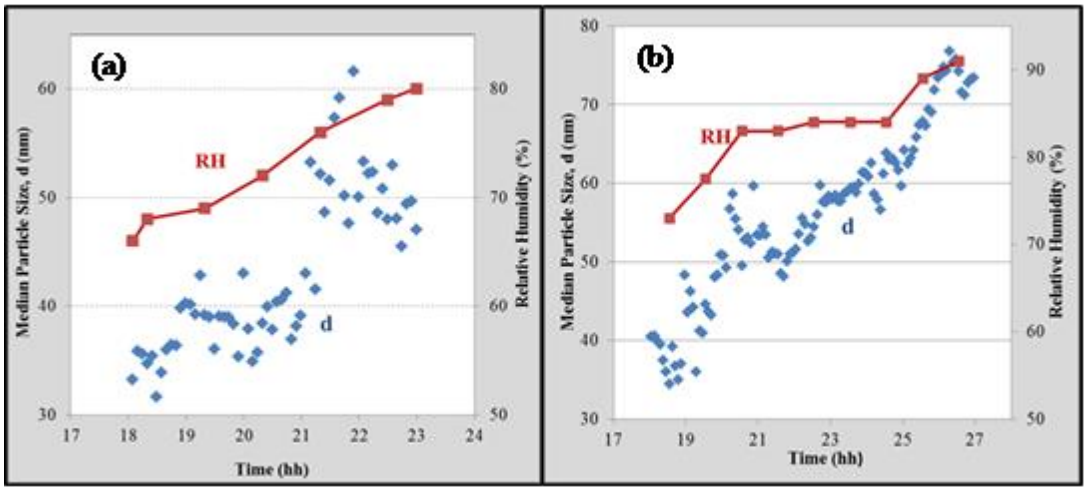

Figure 6: Median particle size and relative humidity as a function of time for growth events on July 16 and July 20, 2012, respectively

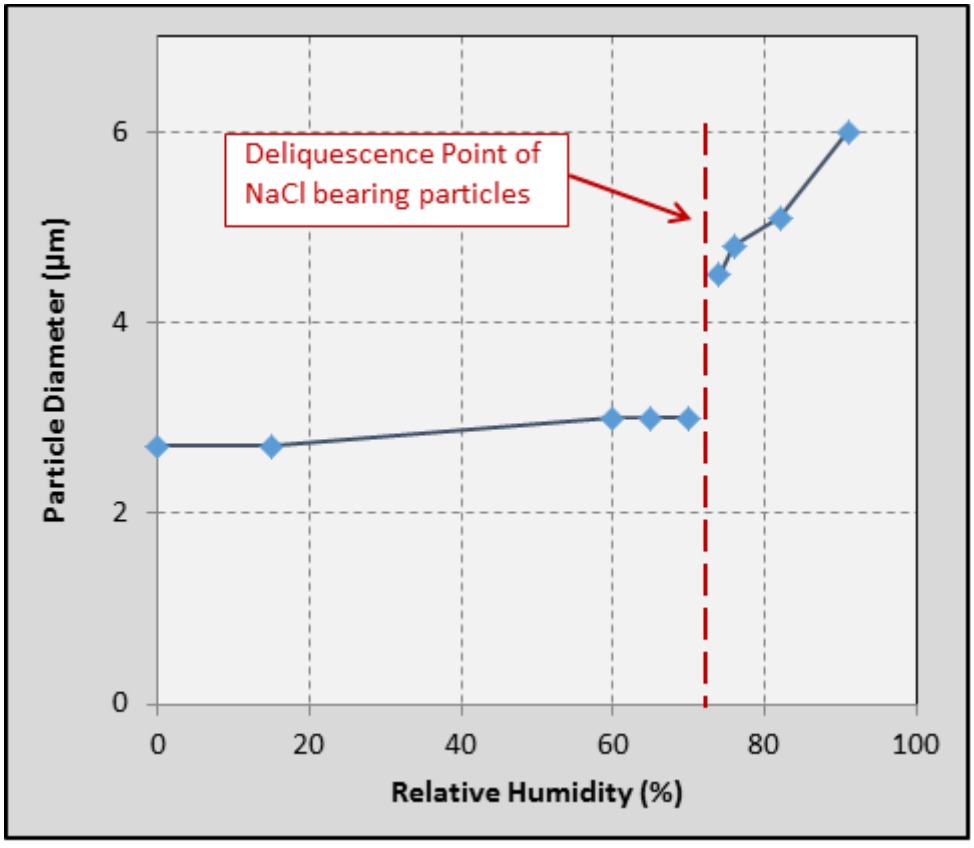

Figure 7: Particle diameter as a function of relative humidity for NaCl-bearing particles. The figure is plotted using the data presented in Wise et al. (2007).

Atmos. Chem. Phys. Discuss., https://doi.org/10.5194/acp-2018-189
Manuscript under review for journal Atmos. Chem. Phys.
Discussion started: 13 April 2018

Atmospheric Chemistry and Physics Discussions

568 **Table 1: Summary of studies reporting night time NPF events**

569 SMPS: Scanning mobility particle sizer, AIS: Air ion spectrometer, BSMA: Balanced scanning mobility

570 analyser, FMPS: Fast mobility particle sizer

Study	Location	Occurrence rate		Instrument (size range)
		Day time	Night time	
Svenningsson et al. (2008)	Abisko, Sweden (characterized by Subartic birch forest)	46/195 days (23%)	31/195 days (16%)	SMPS (10-500 nm) AIS (0.4-40 nm)
Junninen et al. (2008)	Pine Forest, Hyytiala, Finland		344/1279 days (27%)	BSMA (0.4-6.3nm) AIS (0.34-40 nm)
Suni et al. (2008)	Eucalypt forest, Tumbarumba, Australia	184/351 days (52%)	112/351days (32%)	AIS (0.34-40 nm)
Kalivitis et al. (2012)	Finokalia, Lassithiou, Greece (remote coastal site)	53/365 days (15%)	39/365 days (11%)	SMPS (9-900 nm) AIS (0.8-42 nm)
Man et al. (2015)	Suburban coastal site, Hong Kong	12/112 days (11%)	5/112 days (4%)	FMPS (5.6-560 nm)
Mazon et al. (2016)	SMEAR II, boreal forest, Hyytiala, Finland		using neg ions: 1324/4015 days (34%) using pos ions: 1172 /4015 days (30%)	BSMA (0.8-8 nm)

Salimi et al. (2017)	25 sites across Brisbane (characterized by urban environment)	146/285 days (51%)	73/285 days (26%)	SMPS (9-414 nm)
Kammer et al. (2017)	Landes forest, France	2/16 days (12.5%)	6/16 days (37.5%)	SMPS (10-478 nm)

Atmos. Chem. Phys. Discuss., https://doi.org/10.5194/acp-2018-189
Manuscript under review for journal Atmos. Chem. Phys.
Discussion started: 13 April 2018

Atmospheric Chemistry and Physics Discussions

589 Table 2: Summary of the day time and night time NPF events

590

Year	Total Data Available Days	Strong NPF events			Weak NPF events			Total NPF events		
		Day time	Night time	Total	Day time	Night time	Total	Day time	Night time	Total
2012	253	97	7	104	9	9	18	106	16	122
2015	65	18	4	22	5	7	12	23	11	34
2017	167	44	7	51	16	13	29	60	20	80
Total Events		159	18	177	30	29	59	189	47	236
Total days	485	159	18	177	30	29	59	181	47	213
Occurrence rate (%)		33	4	37	6	6	12	37	10	44

591

592

593

594

595

596

597

598

599

600

601

602

603

604

Atmos. Chem. Phys. Discuss., https://doi.org/10.5194/acp-2018-189
Manuscript under review for journal Atmos. Chem. Phys.
Discussion started: 13 April 2018

Atmospheric Chemistry and Physics Discussions

605 Table 3: The mean and the range of meteorology and gas phase parameters on NPF and non-event days

Parameter	Winter Months		Summer Months		NPF days	non-event days
	NPF days	non-event days	NPF days	non-event days		
			Meteorology			
Solar radiation (Wm^{-2})	346 (230-490)	316 (95-476)	600 (202-818)	476 (68-818)	505 (202-818)	397 (68-818)
Temperature (^0C)	17 (12-19)	16 (12-25)	24 (18-29)	24 (19-32)	21 (12-29)	20 (12-32)
Relative Humidity (%)	59 (31-73)	70 (27-90)	52 (23-73)	63 (25-86)	54 (23-73)	66 (25-90)
Wind direction (^{o})	215 S-SW	203 S-SW	197 S-SW	177 S-SW	205 S-SW	200 S-SW
Wind Speed (ms^{-2})	0.38 (0.1-1.1)	0.42 (0.1-1.3)	0.57 (0.1-1.7)	0.81 (0.1-2.1)	0.5 (0.1-1.7)	0.62 (0.1-2.1)
			Gas Phase			
Visibility (Mm^{-1})	15 (6-42)	34 (2-112)	19 (7-41)	29 (6-114)	18 (6-42)	31 (2-114)
Ozone (ppb)	12 (1-29)	10 (2-26)	20 (1-32)	19 (3-35)	17 (1-32)	15 (2-35)
SO_2 (ppb)	7 (6-10)	6 (1-9)	5 (1-14)	3 (1-9)	6 (1-14)	5 (1-9)

606

607

608

Atmos. Chem. Phys. Discuss., https://doi.org/10.5194/acp-2018-189
Manuscript under review for journal Atmos. Chem. Phys.
Discussion started: 13 April 2018

Atmospheric Chemistry and Physics Discussions

609 Table 4: Summary of the growth events, which did not follow the NPF events, obtained using the NAIS

610 data.

Year	Total Data Available Days	Growth Events		
		Day time	Night time	Total
2012	253	24	59	83
2015	65	4	21	25
2017	167	26	55	81
Total events		54	135	189
Total days	485	54	135	179
Occurrence rate (%)		11	28	37

611

612

613

614

615